Hindawi
Mathematical Problems in Engineering
Volume 2022, Article ID 4173457, 15 pages
https://doi.org/10.1155/2022/4173457

Research Article

Numerical Simulation on Optimization of Process Parameters for Free Bending of Metal Tubes

Xinju Zhang, Deshun Su, Jianwei Jin, Zhiqiang Zhou, Zhanpu Xue, Zhenlu Tian, Hao Zhang, Yonglei Shi, and Haipeng Yan

School of Mechanical Engineering, Hebei University of Science and Technology, Shijiazhuang 050018, China

Correspondence should be addressed to Zhanpu Xue; shenghuo166@163.com

Received 14 August 2022; Revised 24 September 2022; Accepted 27 September 2022; Published 3 November 2022

Academic Editor: Ivan Giorgio

Three-dimensional free bending is a new tube forming technology with continuous variable curvature. In order to improve the forming quality of tube, this paper studies the principle of three-dimensional free forming system and the numerical calculation of bending moment in detail, and it uses the finite element simulation to model the mechanism in the bending process. The simulation model is used to simulate the forming process of copper tube, and the influence of key process parameters on the forming process is analyzed,the shape of the inner cavity of the bending die and the gap between the tube and the bending die are studied, the distance between the bending die and the guide column is studied, the axial feed rate on the forming quality of tubular bending parts has also been studied. The optimum process parameters were determined by finite element simulation and analysis.

1. Introduction

Tube structure is an important component for bearing and transporting gas and liquid in the industrial field. It is widely used in aerospace, ships, vehicles, petrochemical industry, construction medical devices, and other fields. Because of its light weight, high strength, high stiffness, and low consumption, it is used to meet the development trend and requirements of lightweight, high performance, and complexity of industrial components [1, 2].

The traditional tube bending technology includes roll bending, bending, and so on. Although it can realize the bending forming of tube, it cannot realize the bending of variable curvature arc tube [3]. Three-dimensional free bending technology is an important technical breakthrough in the field of plastic forming in recent years. It combines multi-axis linkage control technology with traditional tube bending technology, which can ensure the accurate forming of tubes under various conditions of variable curvature bending radius [4]. The real-time change of tube bending radius can be realized without frequent die replacement. These advantages make three-dimensional free bending a flexible forming technology for efficient and accurate manufacturing.

In order to analyze the stress-strain distribution and tube forming quality in tube bending, the numerical method based on nonlinear finite element analysis is usually used to replace the high-cost and time-consuming physical experiment. The finite element analysis method can well simulate the complex forming process, the contact between multiple objects, and the highly nonlinear material behavior in the forming and unloading process, which provides a knowledge basis for mechanical structure design and exploring the optimal forming process parameters.

Finite element analysis is widely used in pipe forming. The process of shear bending of steel pipe is introduced. In addition, elastic-plastic three-dimensional finite element simulation was carried out to analyze the forming process [5]. The shear bending process of circular tube is experimentally studied. In addition, elastic-plastic three-dimensional finite element simulation is carried out to clarify the forming mechanism [6]. In order to accurately predict the wall thickness thinning during pipe bending, considering the change of elastic modulus, a finite element model for NC

bending of high-strength 21-6-9 stainless steel pipe (21-6-9-hs pipe) was established. Using this model, the influence of process parameters on the wall thinning of 21-6-9-hs tube by NC bending is studied [7]. At present, there is no feasible method to provide detailed information about the strain distribution without significantly delaying the planning process, so as to reduce the thickness of the bending zone in the roll forming process. Therefore, a numerical modeling method combining global model and submodel is proposed to achieve high-resolution strain distribution in bending zone at acceptable computational cost [8]. The bending behavior of special-shaped pipe in wall thickness variation and section distortion is studied by simulation and experiment. Experiments were carried out to study bending characteristics, such as wall thickness variation [9]. In the process of bending, the pipe inside the bend is folded and thickened, and the pipe outside the bend is flat and thinner. The elastic-plastic bending finite element analysis was carried out to observe the deformation characteristics of the curved pipe at room temperature, such as flattening, wall thinning, and wall thickening [10]. In ABAQUS/explicit environment, based on the solution of key technologies such as contact boundary conditions, material property definition, and mesh generation technology, a three-dimensional finite element model of pipe bending process is established [11]. Based on a new method, a flexible bending machine is manufactured. In addition, the key parameters of flexible bending of rectangular copper profiles are studied [12].

The flexible bending process of typical asymmetric section angle steel is studied by the finite element analysis method [13]. Using the analysis model, simulation model, and experimental bending results, the forming characteristics of small bending radius elbow based on spherical connection structure are studied [14]. A three-dimensional finite element model of hydroforming process in square section die is established by using dynamic and static methods to study the effects of friction conditions on plastic flow and residual stress [15]. The manufacturing process of exponentially hardened thin-walled tube was studied. The analysis is based on the feedback analysis of bending springback test [16]. The plane strain assumption and exponential hardening law are used to study the plastic deformation of pipes during bending [17]. The three-dimensional elastic-plastic finite element model of square TA18 titanium alloy pipe is established based on ABAQUS/explicit [18], and the distribution and stress-strain changes of the pipe are analyzed. Wall thickness thinning is one of the key defects that determine the forming quality and limit in pipe bending. An analytical model is proposed to reveal the essential relationship between pipe parameters and wall thickness distribution [19]. Incremental tube forming is a combination of free bending and spinning. In order to predict the effect of radial and circumferential superimposed stress generated by spinning roller on bending moment, an analytical model is proposed [20].

In this paper, the free bending process of H62 brass tube is simulated by ABAQUS software, and the stress-strain distribution in the free bending process is analyzed. Through the finite element simulation of the free bending forming process, the rationality of the designed free bending forming die can be effectively verified, the best forming process parameters can be explored, the plastic deformation law of materials in the free bending forming process can be revealed, the process parameters such as the shape of the inner cavity of the bending die, the gap between the tube and the bending die, the distance between the bending die and the guide column can be related to them. The tube feeding speed affected the wall thickness change and stress-strain distribution in the tube forming process, it improved the tube forming quality and forming accuracy, and played a strong guiding role in the die design and the optimization of forming process parameters.

2. Methodology

2.1. Three-Dimensional Free Bending Technology. The principle of three-dimensional free bending forming system is shown in Figure 1, which is mainly composed of tube, bushing, bending die, guide column, and pusher. In the free bending forming process of the tube, after the tube is pressed by the pressing device, the z-direction stepping motor will drive the pushing device to push the tube into the bending die. At the same time, the stepping motor of the X-Y platform will drive the ball die bushing to offset a certain distance in the X-Y direction, and the bending die will also rotate an angle with it. At this time, the z-direction stepping motor will drive the tube to feed to complete the bending forming.

In the initial state of the guide column and the bending die, the central axis is on the same horizontal line. When the X-Y platform is offset, the offset of the bending die is U, the distance between the center of the bending die and the front end of the guide column is A, and the feeding speed of the tube in Z direction is V. In the course of the row, a does not change, and the size of the offset u is determined by the motion of the X-Y platform. At the same time, the size of the bending radius R is determined by U and A, where

$$R = \frac{U^2 + A^2}{2U}. \tag{1}$$

2.2. Calculation of Bending Moment. In order to simplify the analysis of tube bending deformation process, only tangential deformation is considered, the displacement of neutral layer is ignored, and the strain at any strain point in all directions can be expressed as $\varepsilon_\theta = \ln(1 + R \sin \varphi/\rho)$, and the stress expression in the elastic deformation stage is

$$\sigma_\theta = E\varepsilon \; \sigma_\theta < \sigma_s, \tag{2}$$

where E is the modulus of elasticity and ε is the elastic strain.

The expression of stress in plastic deformation stage is

$$\sigma_\theta = K\varepsilon^n \; \sigma_\theta \geq \sigma_s, \tag{3}$$

where K is the strength coefficient, ε is the plastic strain, and n is the hardening index.

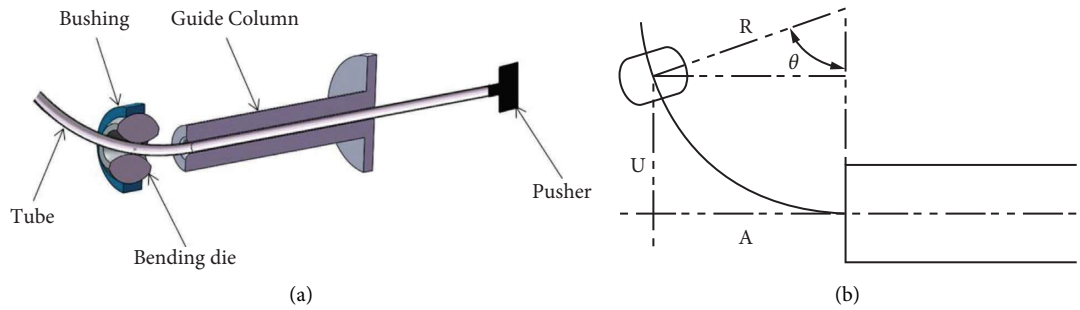

Figure 1: Schematic diagram of three-dimensional free bending forming. (a) Simplified model diagram of 3D free bending. (b) Simplified diagram of bending forming method.

The moment when the tube is bent consists of the moment M_1 required for elastic deformation and the moment M_2 required for plastic deformation. The moment expression is

$$\begin{aligned} M &= M_1 + M_2, \\ M &= 4\int_0^{\varphi a} \sigma_\theta R\sin_\varphi \, trd_\varphi + 4\int_{\varphi a}^{\pi/2} \sigma_\theta R\sin_\varphi \, trd_\varphi, \end{aligned} \tag{4}$$

where R is the tube bending radius, ρ is the curvature radius of tube bending neutral layer, φ is included angle between any point of tube and X-axis, and t is the wall thickness of tube.

Substitute the formula into the equation:

$$\begin{aligned} M = {} & 4\int_0^{\varphi a} E\,\ln\left(1+\frac{R\,\sin\,\varphi}{\rho}\right)R\,\sin_\varphi \, trd_\varphi \\ & + 4\int_{\varphi a}^{\pi/2} K\left(\ln\left(1+\frac{R\,\sin\,\varphi}{\rho}\right)\right)^n R\,\sin_\varphi \, trd_\varphi. \end{aligned} \tag{5}$$

When the tube is in the elastic deformation stage, the deformation of the tube is very small. At this time, the tangential strain of the tube is very small, and $\varepsilon_\theta = \ln(1 + R\,\sin\,\varphi/\rho)$ can be simplified to $\varepsilon_\theta = R\,\sin\,\varphi/\rho$. Bring it into the formula:

$$M = \frac{ER^3 t\,(2\varphi - \sin\,2\,\varphi)}{\rho} + 4Ktr^2\int_{\varphi a}^{\pi/2}\left(\ln\left(1+\frac{R\,\sin\,\varphi}{\rho}\right)\right)^n \sin_\varphi \, d_\varphi. \tag{6}$$

Angle between elastic deformation zone and Z-axis:

$$\begin{aligned} \frac{\sigma_s}{E} &= \frac{R\,\sin\,\varphi_a}{\rho}, \\ \varphi_a &= \arcsin\left(\frac{\rho\sigma}{RE}\right). \end{aligned} \tag{7}$$

3. Definition of Geometric Model and Mesh

Pipe bending is the result of the joint action between parts. Considering the actual working condition of the pipe bender and the calculation speed and efficiency of the software, only six parts of bending die, bushing, guide column, pusher, pipe, and clamping mechanism are modeled. The bushing is simplified and defined as a rigid body to improve the calculation speed. In order to realize the follow-up setting of the bending die, the bending die is set as a deformation body. The guide column and pipe clamping mechanism are to position and clamp the pipe in the bending process to prevent axial instability and buckling of the pipe. It will always be in a static state in the bending process, so it is defined as a rigid body. The pipe will be bent in the forming process, which is defined as a deformable body, and the corresponding material properties are given, such as elastic modulus, density, and tensile strengthan.. In the whole model, the material of the pipe is set as H62 brass, the material of the bending die is bearing steel, and the other parts are Q235 steel.

The type and size of mesh generation affect the efficiency and accuracy of the calculation results. Because the quadrilateral four-node shell element S4R can control the hourglass and reduce the integral, S4R is used to describe the bending forming of pipe. The pushing head, bending die, and guide mechanism are divided by hexahedral eight-node element c3d8r. The bushing is meshed by ten-node modified quadratic tetrahedral element c3d10m. At the same time, if the mesh size of the bending die and the bushing is too large, sharp meshes will appear in the fillet. In order to avoid collision and interference between the bending die and the bushing during the simulation rotation after meshing, it is necessary to divide the mesh size of the bushing and the bending die smaller. Here, the mesh size is 1×1 mm. This element has less sensitivity to mesh distortion and can be applied to numerical analysis of thin shell structure, as shown in Figure 2.

4. Boundary Condition

The bending of the tube is formed by driving the bending die to rotate through the XY platform. The force on the tube is transmitted by the bending die. When the z-axis is fed, the tube will have sliding friction contact with the inner wall of the bending die and the inner wall of the guide column. Therefore, it is necessary to define the interaction between the tube and the two. The interaction between the tube and the inner wall of the universal ball mold and the inner wall of the guide column is set as global universal contact, tangential contact in contact attributes is defined as frictional contact, and the friction coefficient is set as 0.02 (the tube and the

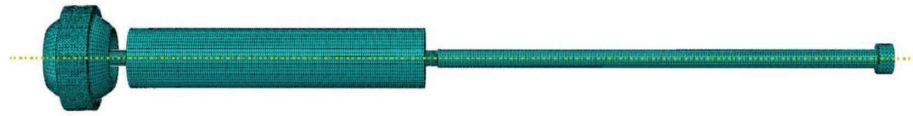

Figure 2: Model meshing.

inner wall of the universal ball mold and the inner wall of the guide column are lubricated with lubricating oil).

During modeling, the bushing, guide column, push head, and clamping mechanism are defined as rigid bodies, and the load cannot be applied to the rigid bodies in ABAQUS. Therefore, a reference point should be established for each rigid body and the load should be applied to the reference point. The universal ball mold rotates with the movement of the bushing, so it only needs to be constrained as a rigid body without loading on the universal ball mold. Set the guide column and clamping mechanism to be fixed, apply the speed in X and Y directions to the bushing reference point, and apply the speed in Z direction to the push head reference point. The load application is shown in Figure 3.

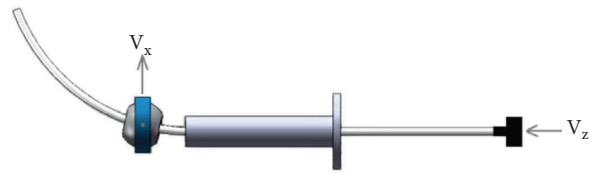

Figure 3: Load application.

5. Numerical Results and Discussion

5.1. Response of Inner Cavity Shape of Bending Die to Tube Forming. The inner cavity shape of bending die is the main factor to describe the contact forming between tube and die in the process of free bending. In the bending forming process, the bending of the tube is mainly formed by sliding contact with the inner cavity of the bending die. In the forming process, it is mainly through line to line contact, which directly affects the deformation conditions and material fluidity of the tube in the forming process. If the design of the inner space of the universal ball is unreasonable, it will directly affect the forming limit and forming quality of the tube.

The six cases of $r = 5$ mm, $r = 10$ mm, $r = 15$ mm, $r = 20$ mm, $r = 25$ mm, and $r = 30$ mm will be studied. As shown in Figure 4, when the arc radius of the inner cavity of the bending die is less than 5 mm, the contact area between the tube and the bending die will be too small during bending. When the tube wall thickness is thin, the concentrated stress on the tube will increase, and the tube surface will be concave or broken. It affects the forming quality, so it is not considered.

It can be seen from Figure 5 that with the decrease of the inner cavity radius of the bending die, the bending radius of the tube is gradually increasing, because the arc radius of the inner cavity is more larger, when the tube is bent and fed, the small bendable space in the bending die can hinder the feeding of the tube and the fluidity of the material. At the same time, with the decrease of the inner cavity radius of the bending die, the stress value of the tube is also gradually decreasing. When the arc radius of the inner cavity is 30 mm, the maximum peak stress of the tube is 559.5 Mpa. When the arc radius of the inner cavity is 5 mm, the maximum peak stress of the tube is 538.2 Mpa. This is because with the decrease of the arc radius of the inner cavity, the bendable space provided to the tube increases and the material fluidity is smoother. When the tube is fed, the influence of material accumulation is gradually reduced, the instantaneous stress value is also reduced, the bending degree of the tube is gradually increased, and the quality is also improved.

The change of inner and outer wall thickness of the tube is shown in Figure 6. It can be seen from Figure 6 that when the half radius of the inner cavity arc is reduced from 30 mm to 5 mm, the change rate of the inner and outer arc wall thickness of the tube gradually decreases, but the change of the inner and outer wall thickness of the tube tends to be thickened. This is because with the decrease of the inner cavity arc radius, the material fluidity is smoother. However, there is no gap between the tube and the universal ball mold in the ideal state. During the feeding process, the inner and outer sides of the tube are squeezed by the inner cavity of the bending die at the same time, resulting in the thickening trend of the inner and outer wall thickness. Therefore, it is necessary to further study the gap between the tube and the die.

Therefore, in order to improve the forming quality of tube, the inner cavity radius of bending die is 5 mm.

5.2. Response of Tube Die Gap on Tube Forming. Due to the outer diameter tolerance of the tube during processing, there should be a certain gap Δa between the inner cavity of the ball mold and the outer diameter of the tube, as shown in Figure 7, so as to ensure the smooth entry and bending of the tube. In order to study the influence of the gap between tube and die on the forming quality of tube, the variation range of gap is taken as 0–0.5 mm in this paper. When the gap value is greater than 0.5 mm, the gap is obviously too large, which will have a great impact on the accuracy of tube bending, so it will not be considered.

It can be seen from Figure 8 that with the increase of the gap value, the bending radius of the tube increases gradually. This phenomenon occurs because the gap value is related to the actual eccentricity applied by the universal ball mold to the tube. It is assumed that the eccentricity generated by the movement of the bending die under the driving action of the X-Y platform is U, and the actual eccentricity applied by the bending die to the tube blank is U. Then, $U = U - \Delta a$. With

Figure 4: Inner cavity shape of bending die.

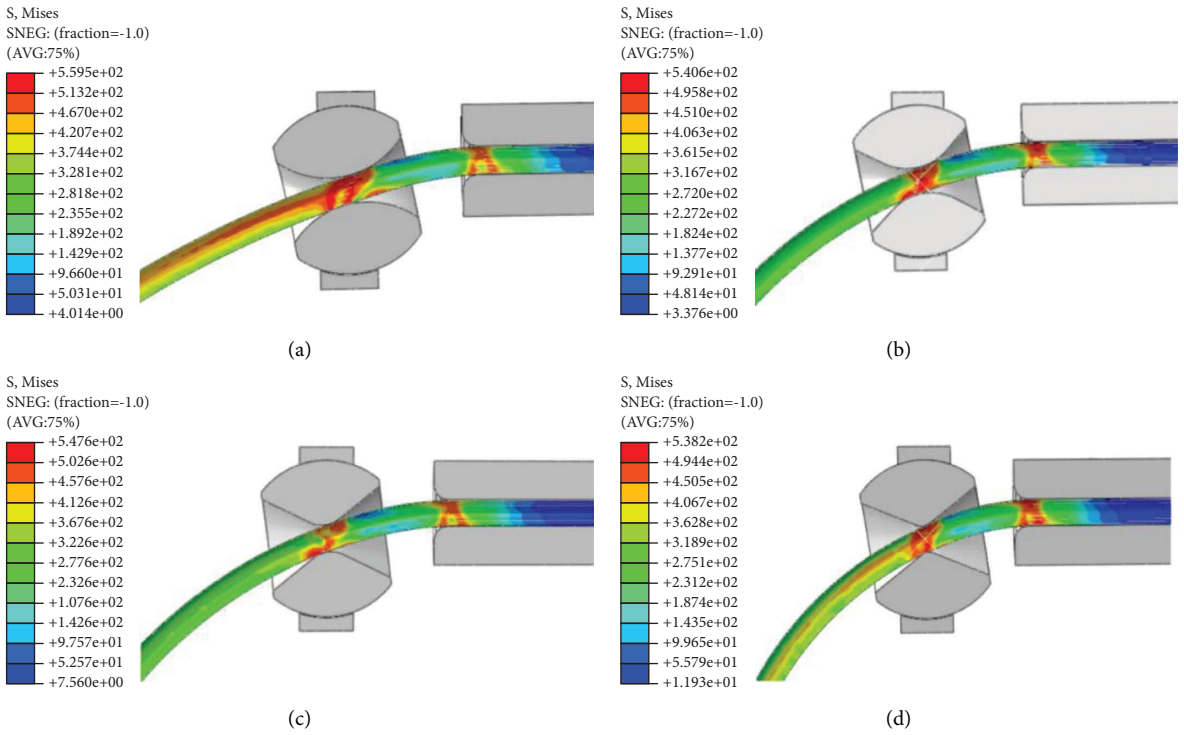

Figure 5: Forming process under different inner cavity radii. (a) Tube stress at $r = 30$ mm. (b) Tube stress at $r = 20$ mm. (c) Tube stress at $r = 10$ mm. (d) Tube stress at $r = 5$ mm.

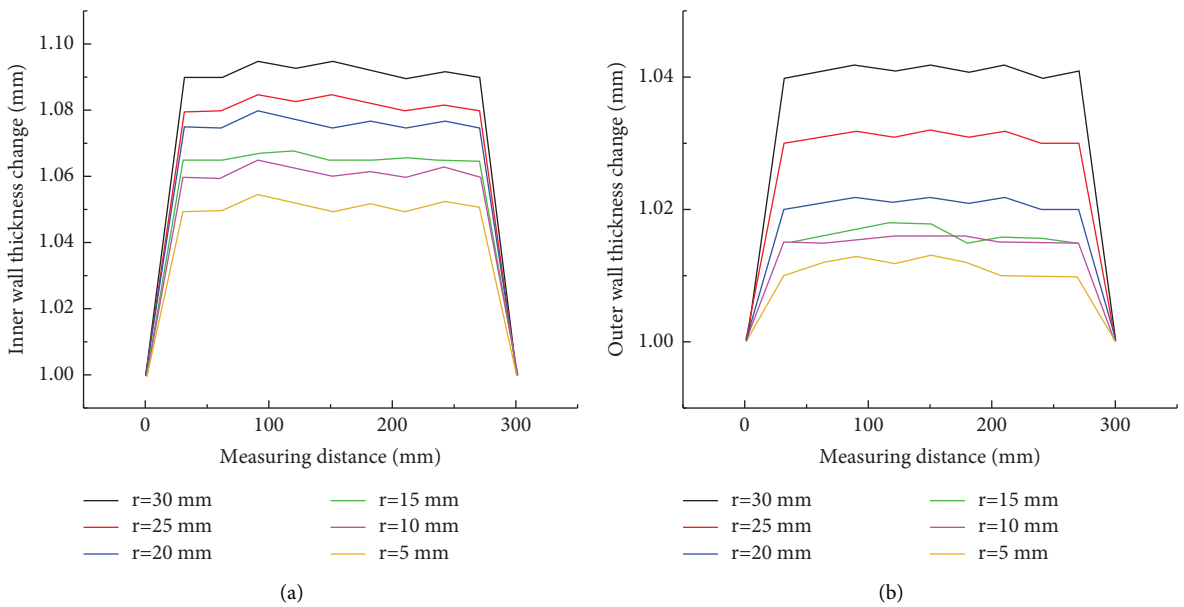

Figure 6: Change of inner and outer wall thickness of tube. (a) Inner wall thickness change. (b) Outer wall thickness change.

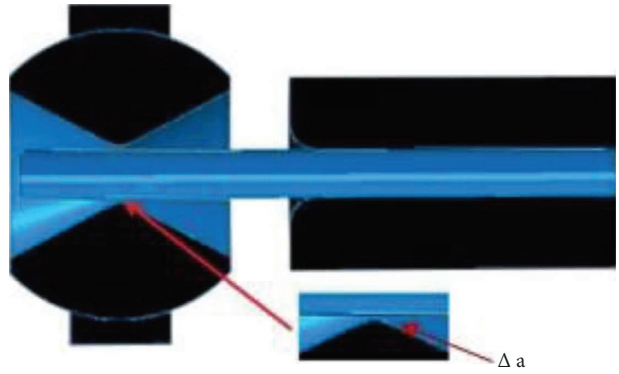

Figure 7: Schematic diagram of tube mold clearance.

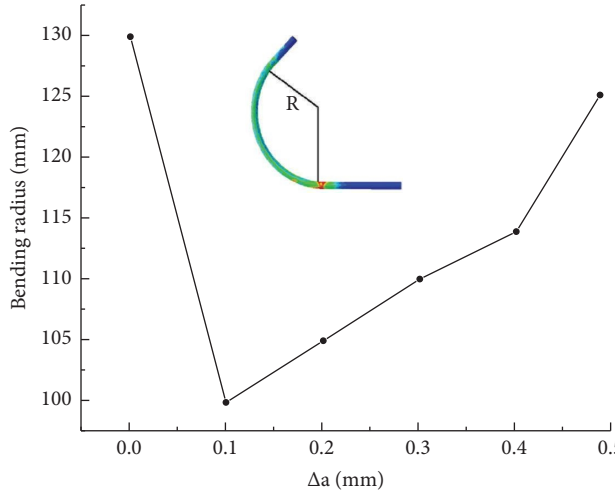

Figure 8: Bending radius under different gaps.

the gradual increase of Δa value, the real eccentricity of the tube decreases gradually, so the bending radius of the tube blank increases gradually.

As can be seen from Figure 9, with the increase of the gap value, the outer wall thickness of the tube decreases gradually because the outer side of the tube is subjected to tensile stress during the forming process, which makes the material thinner under tension. The inner wall thickness of the tube is gradually increasing because the inner side of the tube is under pressure stress during the forming process, which makes the material thicker under pressure. The forming processes of tubes with gap values of 0.1 mm and 0.5 mm are compared, as shown in Figure 10. When the gap value is 0.5 mm, there is a large gap between the inner arc position of the elbow and the bending die. In this case, the trend of tube section distortion cannot be effectively suppressed, resulting in poor forming quality. In addition, when the gap value is large, the forming limit of the tube will be reduced accordingly. Under the same eccentricity, when the gap value is 0.5, the maximum equivalent force on the tube is 510.5 MPa, while when the gap value is 0.1 mm, the maximum equivalent force on the tube is 543.2 MPa. The smaller the gap value is, the greater the degree of bending of the tube is, and the forming limit of the tube is improved accordingly.

However, in the free bending process, if the gap value is too small, the tube section is excessively constrained by the bending die. At this time, the material flow of the tube is blocked, the friction resistance between the tube and the bending die will be greatly amplified, and the surface quality of the tube will become worse. Therefore, in order to improve the forming quality of the tube, the gap between the bending die and the tube is 0.1 mm.

5.3. Response of Bending Deformation Zone Length to Tube Forming. According to the formula $R = U^2 + A^2/2U$, the bending radius r of the tube is determined by the offset u and the distance a between the ball die and the front end of the guide column. The value of a has a great impact on the forming quality and accuracy of the tube. When the value of a is too large, the bending radius of the tube will become smaller and affect the forming accuracy of the tube. When a value is too small, the bending deformation zone becomes shorter and the bending radius of the tube increases, but the front end of the tube and the guide column will produce large stress concentration and affect the forming quality. Therefore, it is necessary to study the size of a value and determine the optimal value through finite element simulation.

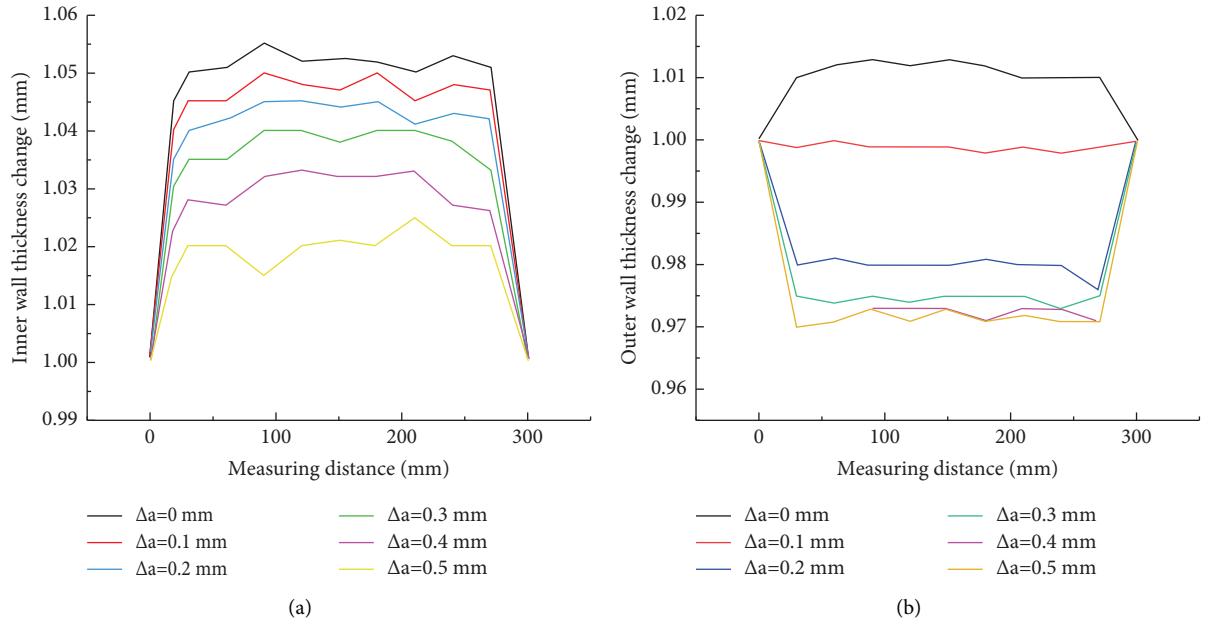

Figure 9: Change of inner and outer wall thickness of tube. (a) Inner wall thickness change. (b) Outer wall thickness change.

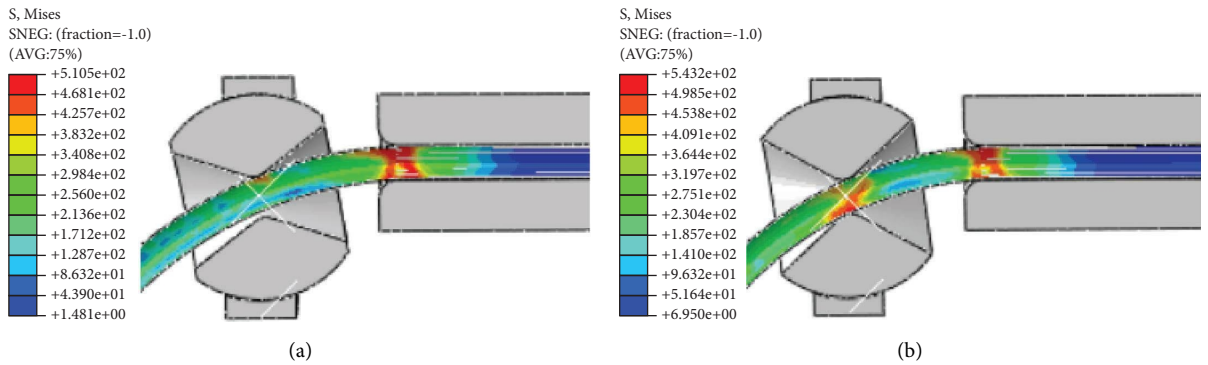

Figure 10: The tube forming process is compared. (a) Tube stress at $\Delta a = 0.1$ mm. (b) Tube stress at $\Delta a = 0.5$ mm.

In the NC tube bender used in this study, the maximum outer diameter of the bending die is 30 mm. In order to avoid collision with the guide column during rotation, the minimum distance between the center of the bending die and the front end of the guide column is 30 mm.

In this paper, the value of a is set in the range of 30 mm–44 mm. When the value of a is greater than 44 mm, the distance at this time is not enough to interfere with the rotation of the bending die in the forming process, but too large a value will have a great impact on the forming accuracy and forming quality, so it will not be considered.

It can be seen from Figure 11 that the bending radius r of tube increases with the increase of a value because according to the forming principle formula $R = U^2 + A^2/2U$, when the offset is certain, the larger the a value, the larger the forming radius R.

In order to accurately measure the influence of a value on tube forming accuracy, the equivalent stress nephogram of tube three-dimensional free bending simulation results corresponding to different A values under the same feeding length and eccentricity is obtained, and the unit is Pa, as shown in Figure 12. From the perspective of equivalent stress, the peak stress in the free bending process decreases with the increase of A value. This is because under the condition of a certain offset, the larger the A value, the smaller the tube forming radius, and the bending moment required for tube bending also decreases.

The change of wall thickness of inner arc and outer arc of tube is shown in Figure 13. It can be seen that when a value increases from 30 mm to 44 mm, the change rate of wall thickness of inner arc and outer arc of tube decreases gradually. This is because the bending radius of the tube gradually increases with the increase of a value, and the bending deformation degree of the tube gradually decreases.

To sum up, the value of A is 34 mm.

5.4. Response of Feed Speed on Tube Forming. In the process of free bending, the forming size of tube bending is mainly determined by the offset U of bending die and the feed

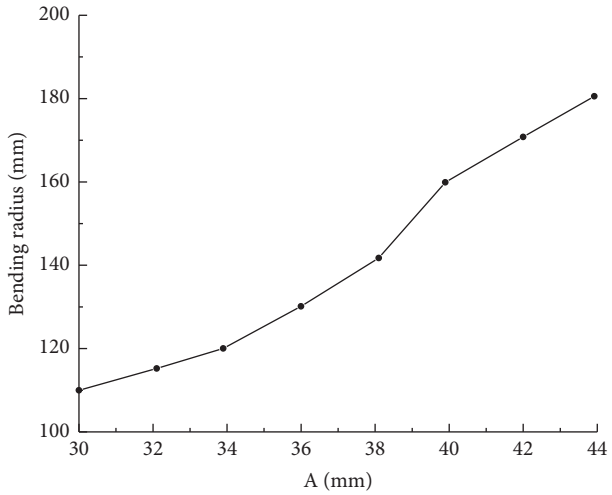

Figure 11: Bending radius at different A values.

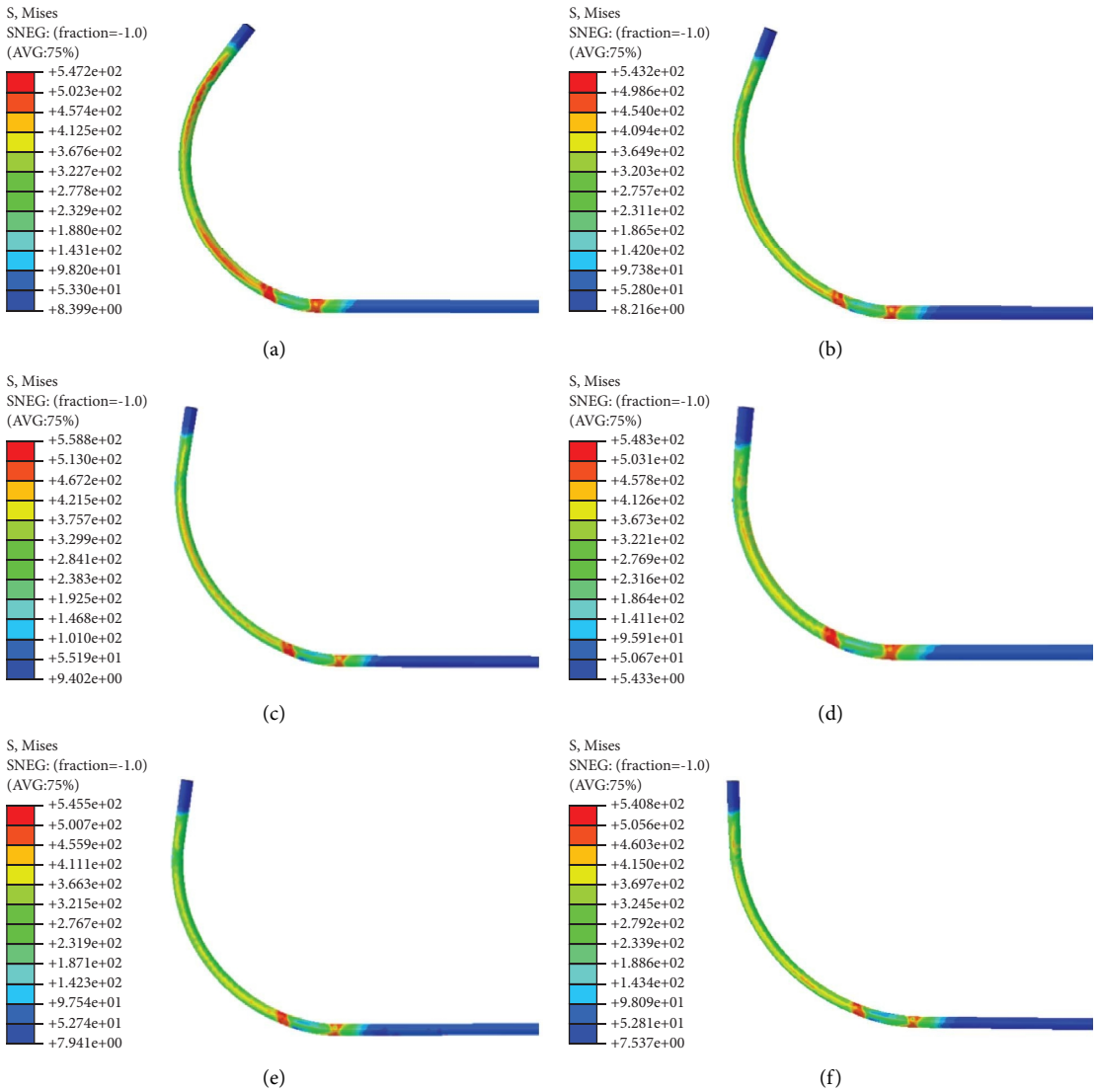

Figure 12: Continued.

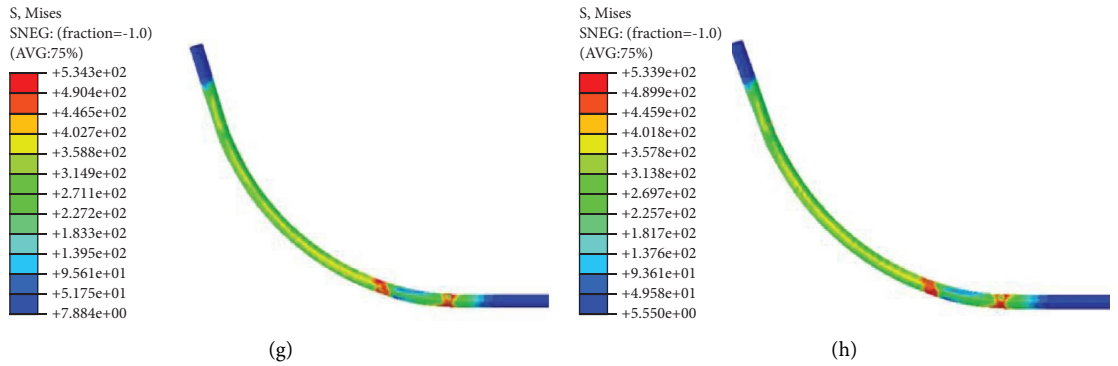

Figure 12: Nephogram of equivalent force under different a values. (a) Tube stress at $A = 30$ mm. (b) Tube stress at $A = 32$ mm. (c) Tube stress at $A = 34$ mm. (d) Tube stress at $A = 36$ mm. (e) Tube stress at $A = 38$ mm. (f) Tube stress at $A = 40$ mm. (g) Tube stress at $A = 42$ mm. (h) Tube stress at $A = 44$ mm.

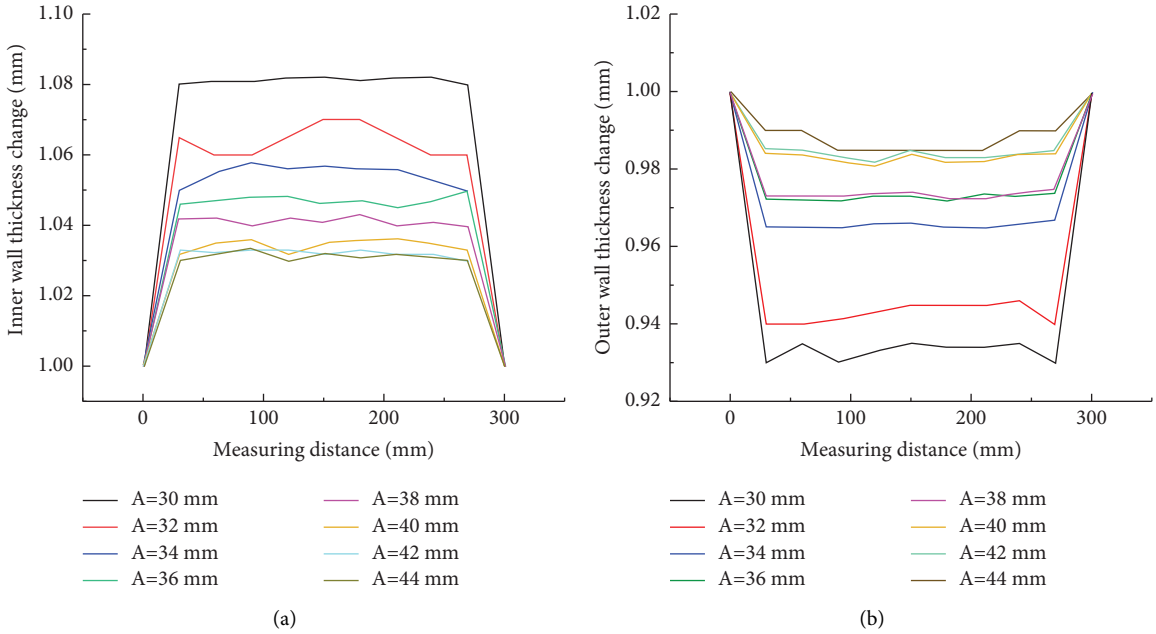

Figure 13: Change of wall thickness of inner arc and outer arc of tube. (a) Inner wall thickness change. (b) Outer wall thickness change.

length of tube, and the feed speed of tube can be adjusted in a large range. The faster the feed speed, the higher the efficiency of tube forming. With the increase of feed speed, the strain rate of tube will also increase. In this case, the resistance of the material will also increase, and the phenomenon of material accumulation and local stress concentration may occur on the tube surface. During the feeding process, tube bending, buckling, and instability may even occur, resulting in the failure of smooth forming of the tube.

The feed speed of tube is set as 10 mm/s, 20 mm/s, 30 mm/s, 40 mm/s, and 50 mm/s, the influence of feed speed on forming results is studied, and the offset is consistent with the feed length. The results are shown in Figure 14.

As can be seen from Figure 13, when comparing the four cases of $V = 10$ mm/s, $V = 20$ mm/s, $V = 30$ mm/s, $V = 40$ mm/s, and $V = 50$ mm/s, it can be seen that with the continuous increase of feed speed, the bending radius of tube is increasing, and the forming quality is also deteriorating. Compared with $V = 10$ mm/s and $V = 20$ mm/s, the forming quality of tube is better, and the shape of forming arc is close to that of standard arc. From the perspective of equivalent stress, when $V = 10$ mm/s, the stress value in the bending deformation zone is small in the bending section of the tube, and the forming quality is good. When $V = 20$ mm/s, the stress concentration in the bending deformation zone is distributed on the inner side of the bending section, and the axial propulsion speed has little effect on the peak stress in the bending deformation zone.

At the same time, by comparing the forming quality of the tube at the two feed speeds of $V = 30$ mm/s and $V = 40$ mm/s, it can be found that when the feed speed is greater than $V = 30$ mm/s, the curved arc shape of the tube has been significantly deformed. This is because the

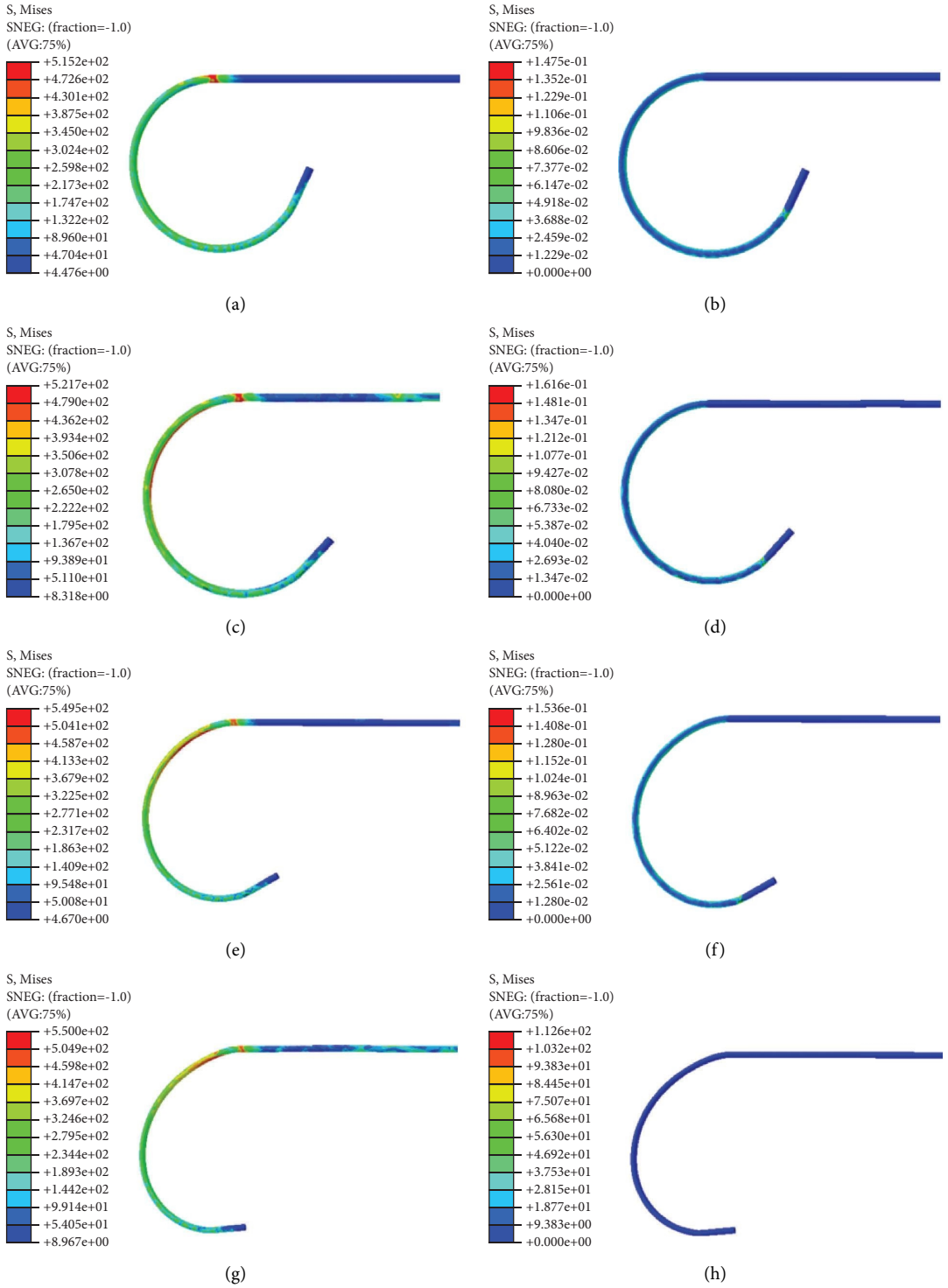

Figure 14: Continued.

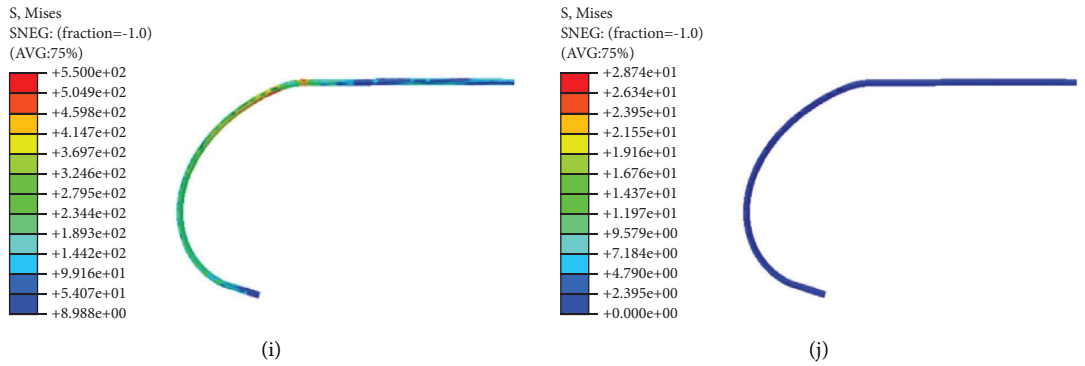

Figure 14: Stress-strain diagram of tube under different feed speeds. (a) Stress diagram at $V = 10$ mm/s. (b) Strain diagram at $V = 10$ mm/s. (c) Stress diagram at $V = 20$ mm/s. (d) Strain diagram at $V = 20$ mm/s. (e) Stress diagram at $V = 30$ mm/s. (f) Strain diagram at $V = 30$ mm/s. (g) Stress diagram at $V = 40$ mm/s. (h) Strain diagram at $V = 40$ mm/s. (i) Stress diagram at $V = 50$ mm/s. (j) Strain diagram at $V = 50$ mm/s.

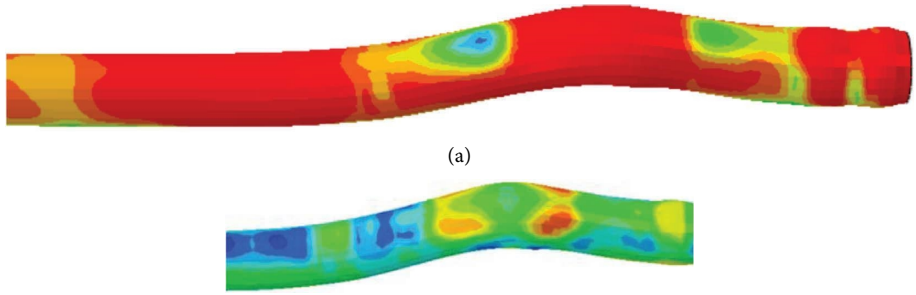

Figure 15: Axial buckling and bending when the advancing speed of tube is too high. (a) Excessive tail end stress. (b) Bend.

Figure 16: CNC tube bender.

tube feed speed is too fast, resulting in local instability and deformation before forming. At the same time, when passing through the bending die, the instantaneous stress of the tube increases, which also leads to the deformation of the bending shape of the tube.

When the axial advancing speed is too high, the resistance of the tube in the bending deformation zone is too large, the normal stress of the cross section of the tube reaches the yield limit of the material, and the tube shows the strength failure of extrusion. As shown in the figure, when the axial length of the tube is large, the axial external load of the tube is greater than the critical load value, and the linear equilibrium state of the tube propulsion section suddenly changes to an unstable state, showing the buckling phenomenon of axial instability. In this paper, when $V = 50$ mm/s as shown in Figure 15, the defect at the end of the tube is strength failure.

In order to improve the tube bending efficiency and forming quality, the axial feed rate should be 20 mm/s.

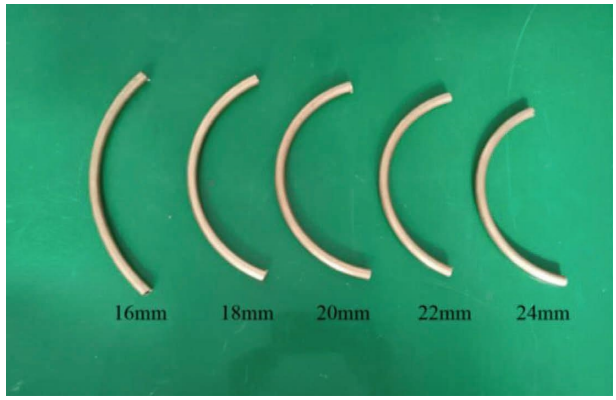

Figure 17: Experimental results of bending forming.

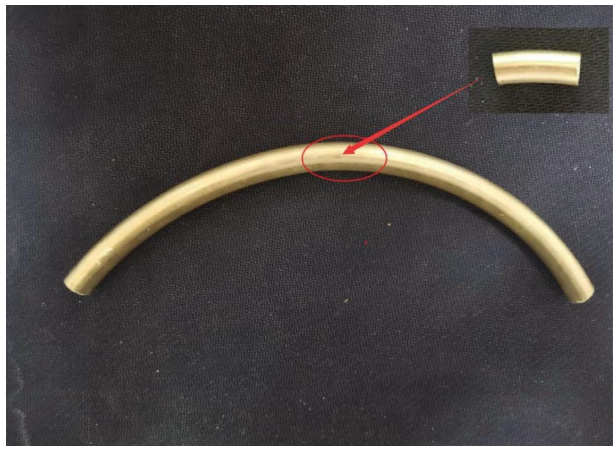

Figure 18: Cutting part.

(a)

(b)

Figure 19: Continued.

(c) (d)

Figure 19: Wall thickness change and section distortion. (a) Inner wall thickness. (b) Outer wall thickness. (c) Minimum tube diameter. (d) Maximum tube diameter.

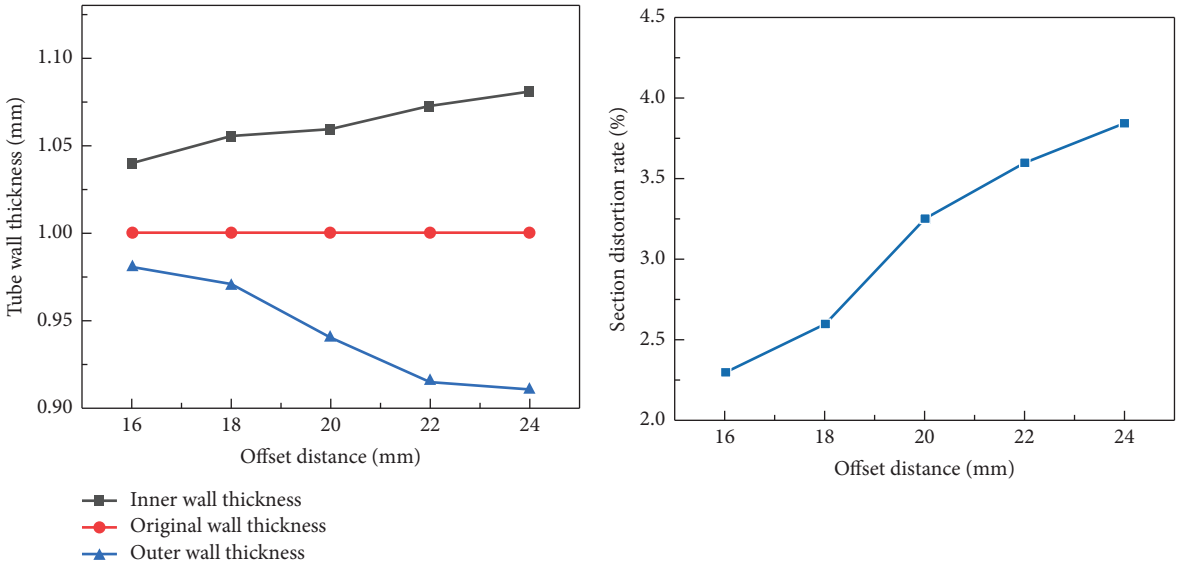

(a) (b)

Figure 20: Wall thickness change and section distortion rate of formed tube under different offsets. (a) Wall thickness change. (b) Section distortion rate.

6. Experiment Verification

In order to verify the accuracy of the orthogonal test results, the free bending equipment is used to bend the tube, and its forming quality is analyzed. The tube bending equipment used in this paper is a CNC tube bender manufactured according to the three-dimensional free bending technology. Its object is shown in Figure 16.

The best forming process parameters are selected by the orthogonal test. Within the bending forming limit of the tube bender, the offset of X-Y axis is set to 16 mm, 18 mm, 20 mm, 22 mm, and 24 mm, respectively. Five groups of bending forming experiments are carried out on the wall thickness change and section distortion of tube bending under different offsets. The forming experimental results are shown in Figure 17.

Wire cut the middle part of the formed elbow, as shown in Figure 18. Measure the wall thickness change and section distortion of the cutting part. The measurement process is shown in Figure 19.

As can be seen from Figure 20, under the optimal forming process parameters, with the increase of offset, within the bending forming limit, the maximum wall thickness thinning rate of the tube is 8%, and the maximum section distortion rate is only 3.8%, which meets the application requirements in the industrial field, and the forming quality is good, indicating the accuracy of the optimal forming process parameters.

7. Conclusion

The three-dimensional free bending technology is used to analyze the stress in the pipe forming process and optimize the forming process parameters of copper pipe, and the conclusions are drawn as follows:

(1) The process of bending tubular parts is analyzed by the mathematical model. The principle of three-dimensional motion is described graphically, which provides an important guidance for the design of the free bending process.

(2) By optimizing the key bending process parameters, such as the inner cavity parameters of the bending die, the gap between the tube and the bending die, the distance between the bending die and the guide column, and the axial pushing speed, the forming quality and accuracy of the tube have been greatly improved.

(3) The gap value has a great impact on the pipe forming quality. In order to form the pipe smoothly, there must be a certain gap. With the increase of the gap value, the pipe forming quality is improved, but the forming accuracy is reduced. When the gap value is 0.1 mm, it is more suitable for forming.

(4) When the feed rate is lower than 20 mm/s, the pipe forming quality is better, but the efficiency is lower. When the feed speed is greater than 20 mm/s, the forming of pipe is prone to instability and distortion, and the pipe has been bent externally with the continuous increase of speed.

Data Availability

The data used to support the findings of this study are available from the corresponding author upon request.

Conflicts of Interest

The authors declare that they have no conflicts of interest.

Acknowledgments

This research was supported by the Foundation of State Key Laboratory of Public Big Data (no. PBD2021-06) and the Natural Science Foundation of Hebei Province (no. E2021208004).

References

[1] M. Hermes, D. Staupendahl, C. Becker, and A. E. Tekkaya, "Innovative machine concepts for 3D bending of tubes and profiles," *Key Engineering Materials*, vol. 473, pp. 37–42, 2011.

[2] C. Zhang, H. Li, and M. Q. Li, "Detailed analysis of surface asperity deformation mechanism in diffusion bonding of steel hollow structural components," *Applied Surface Science*, vol. 371, no. 15, pp. 407–414, 2016.

[3] P. Gantner, D. K. Harrison, S. Akmd, and B. Herbert, "New Bending Technologies for the Automobile Manufacturing Industry," in *Proceedings of the 34th International MATADOR Conference*, Springer, London, U.K, January 2004.

[4] S. Chatti, M. Hermes, A. Tekkaya, and M. Kleiner, "The new TSS bending process: 3D bending of profiles with arbitrary cross-sections," *CIRP Annals*, vol. 59, no. 1, pp. 315–318, 2010.

[5] T. K. Mgoodarzi and M. Murata, "Deformation analysis for the shear bending process of circular tubes," *Journal of Materials Processing Technology*, vol. 162, 2005.

[6] M. Goodarzi, T. Kuboki, and M. Murata, "Effect of die corner radius on the formability and dimensional accuracy of tube shear bending," *International Journal of Advanced Manufacturing Technology*, vol. 35, no. 1-2, pp. 66–74, 2007.

[7] J. Fang, F. Ouyang, S. Lu, K. Wang, and X. Min, "Effect of process parameters on wall thinning of high strength 21-6-9 stainless steel tube in numerical control bending," *Journal of Physics: Conference Series*, vol. 1885, no. 2, Article ID 022033, 2021.

[8] T. Traub, X. Chen, and P. Groche, "Experimental and numerical investigation of the bending zone in roll forming," *International Journal of Mechanical Sciences*, vol. 131-132, pp. 956–970, 2017.

[9] M. Bhargava, S. Kumar, A. Bhatt, B. Simhachalam, and K. Srinivas, "Experimental and simulation studies on bending behaviour of a profile tube," *Advances in Materials and Processing Technologies*, vol. 5, no. 1, pp. 141–152, 2019.

[10] H. S. Jeong, J. W. Jeon, M.-Y. Ha, and J. R. Cho, "Finite element analysis for inconel 625 fine tube bending to predict deformation characteristics," *International Journal of Precision Engineering and Manufacturing*, vol. 13, no. 8, pp. 1395–1401, 2012.

[11] X. B. Xu, T. K. Xiong, Q. Guan, and L. J. Tan, "Finite element simulation and numerical analysis in the process of tube bending," *Advanced Materials Research*, vol. 421, pp. 14–18, 2011.

[12] R. Hashemi and S. A. Niknam, "Flexible bending of rectangular profiles: numerical and experimental investigations," *Journal of Manufacturing Processes*, vol. 56, pp. 390–399, 2020.

[13] P. Li, L. Wang, and M. Li, "Flexible-bending of profiles with asymmetric cross-section and elimination of side bending defect," *International Journal of Advanced Manufacturing Technology*, vol. 87, no. 9-12, pp. 2853–2859, 2016.

[14] X. Guo, H. Xiong, H. Li et al., "Forming characteristics of tube free-bending with small bending radii based on a new spherical connection," *International Journal of Machine Tools and Manufacture*, vol. 133, pp. 72–84, 2018.

[15] A. Ktari, A. Abdelkefi, N. Guermazi, P. Malecot, and N. Boudeau, "Numerical investigation of plastic flow and residual stresses generated in hydroformed tubes," *Proceedings of the Institution of Mechanical Engineers - Part L: Journal of Materials: Design and Applications*, vol. 235, no. 5, pp. 1100–1111, 2021.

[16] E. Daxin and M. Chen, "Numerical solution of thin-walled tube bending springback with exponential hardening law," *Steel Research International*, vol. 81, no. 4, pp. 286–291, 2010.

[17] S. Q. Lu, J. Fang, and K. L. Wang, "Plastic deformation analysis and forming quality prediction of tube NC bending," *Chinese Journal of Aeronautics*, vol. 29, no. 5, pp. 1436–1444, 2016.

[18] C. Liu, X. D. Yan, Y. Yang, and W. Ye, "Research on the springback of square TA18 titanium alloy tube on the numerical simulation," *Materials Science Forum*, vol. 944, no. 2, pp. 753–760, 2019.

[19] J. Fang, F. Ouyang, S. Lu, K. Wang, X. Min, and B. Xiao, "Wall thinning behaviors of high strength 0Cr21Ni6Mn9N tube in numerical control bending considering variation of elastic modulus," *Advances in Mechanical Engineering*, vol. 13, no. 5, Article ID 168781402110212, 2021.

[20] E. Nazari, D. Staupendahl, C. Lobbe, and A. E. Tekkaya, "Bending moment in incremental tube forming," *International Journal of Material Forming*, vol. 12, no. 1, pp. 113–122, 2018.